***Supplementary Materials*: Dose-rate dependence of natural and regenerated TL signals of feldspars extracted from bedrock samples**

N. D. Brown, E. J. Rhodes

1 Ambiguous $T_{1/2}$ values (Fig. S1)

The glow curves from samples J0999, J1008, and J1009 cannot easily be compared with the other samples for determination of $T_{1/2}$ values. Fig. S1 illustrates the reason for this difficulty by comparing the glow curve from J0997 with two curves from J0999. The glow curves of J0999 both exhibit low-temperature shoulders that broadly coincide with the main peak of J0997. Because the shoulders are significantly impacted by the higher temperature peaks, they are not easily separated. Our interpretation is all three of these samples are in significant thermal disequilibrium, meaning that the low-temperature shoulder has only recently become thermally stable and has not had time to grow above the level of the higher temperature peak. This interpretation is borne out in additive dose-response curves (see Brown, 2017).

2 Grain size analysis (Figs. S2 - S4)

The following petrographic thin section images were taken with cross-polarized light at 20 or 100× magnification (see scale bars). Following the analyses of King et al. (2016), grain size estimations were performed using the Digital Grain Size MATLAB package of Buscombe (2013), available at https://github.com/dbuscombe-usgs/DGS.

3 Athermal fading analysis (Figs. S5 - S16)

The following TL measurements were used to estimate the ρ' parameter for each sample, as described in the main text. Note that only the last three $T_{1/2}$ values were used to determine the best-fit ρ' values. The resulting fits are shown (red x symbols), along with the coefficient of determination (R^2) values.

References

Brown, N.D., 2017. Using luminescence signals from bedrock feldspars for low-temperature thermochronology. Ph.D. thesis. University of California, Los Angeles.

Buscombe, D., 2013. Transferable wavelet method for grain-size distribution from images of sediment surfaces and thin sections, and other natural granular patterns. Sedimentology 60, 1709–1732.

King, G.E., Herman, F., Lambert, R., Valla, P.G., Guralnik, B., 2016. Multi-OSL-thermochronometry of feldspar. Quaternary Geochronology 33, 76–87.

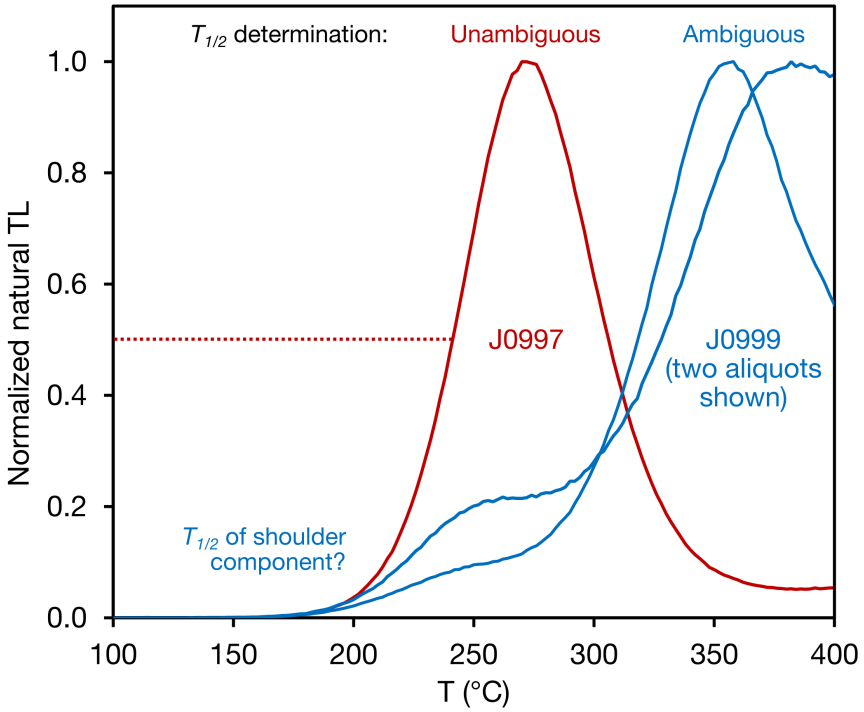

Figure S1: The glow curves of J0997 (red) and J0999 (blue) are shown to have natural peaks or subpeaks between $T = 250 - 300$°C. The $T_{1/2}$ value for J0997 can be readily identified. For J0999, the $T_{1/2}$ value of the relevant subpeak is unclear.

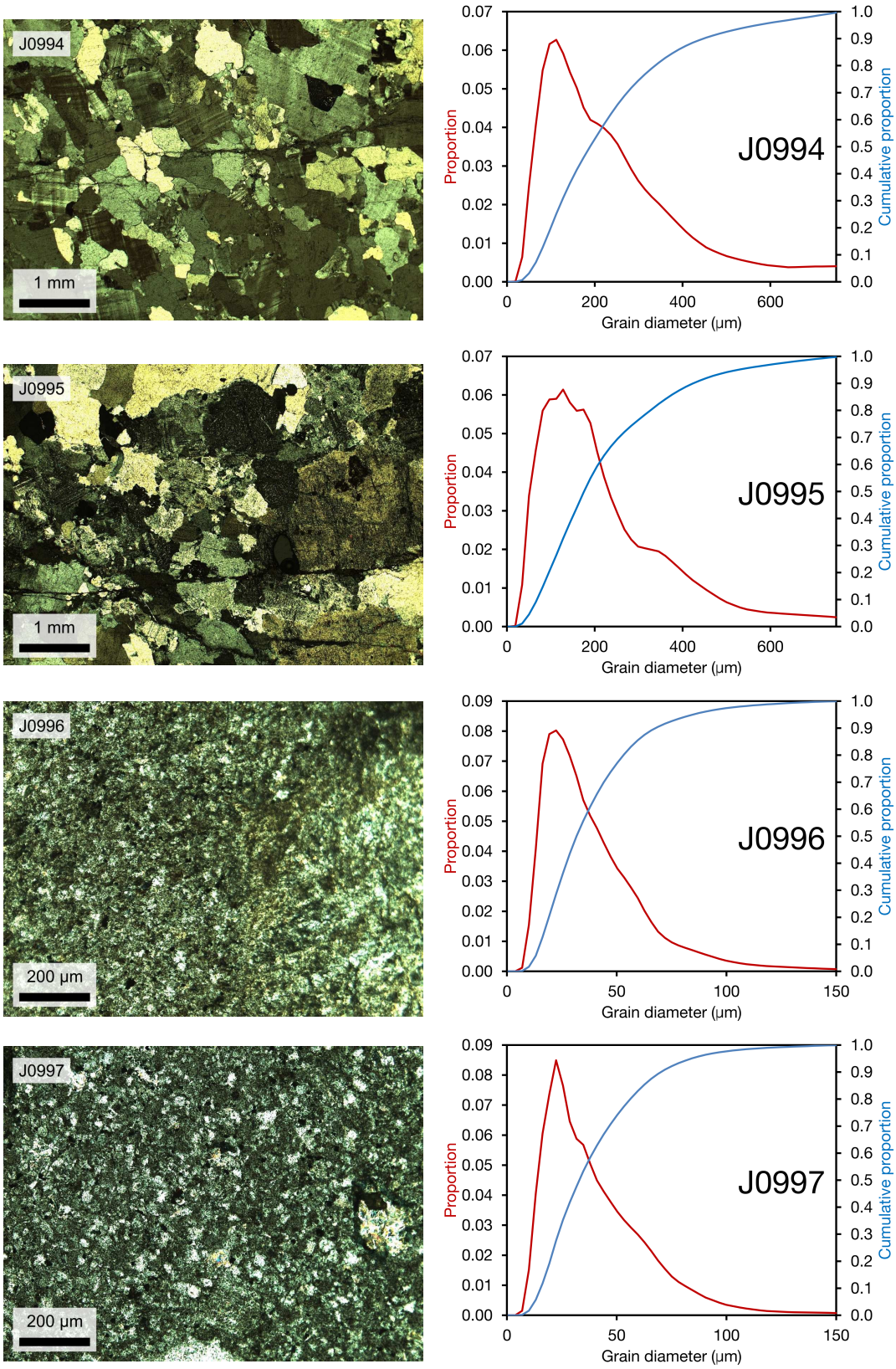

Figure S2: Petrographic thin sections and grain size analysis using DGS (Buscombe, 2013).

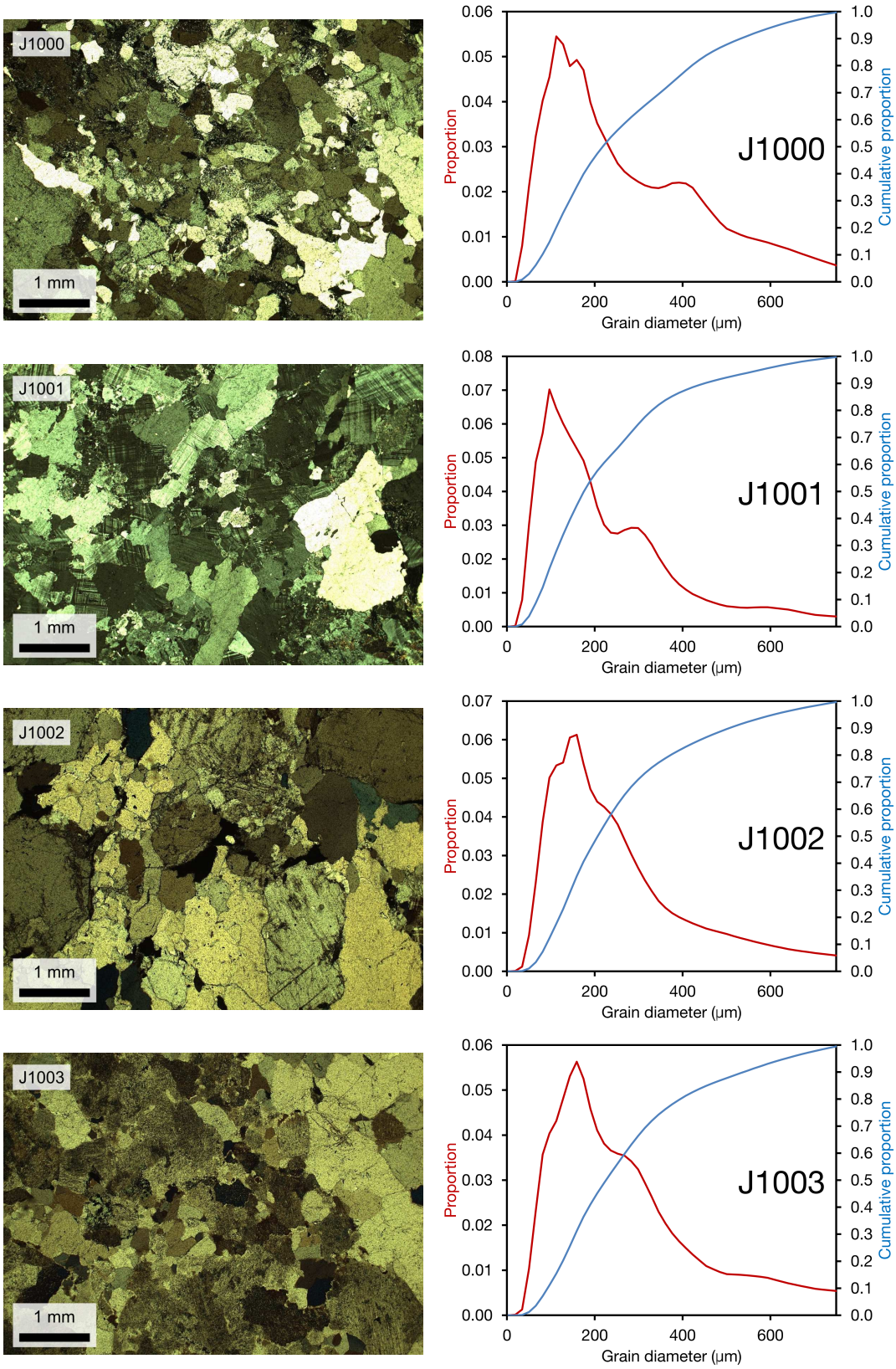

Figure S3: Petrographic thin sections and grain size analysis using DGS (Buscombe, 2013).

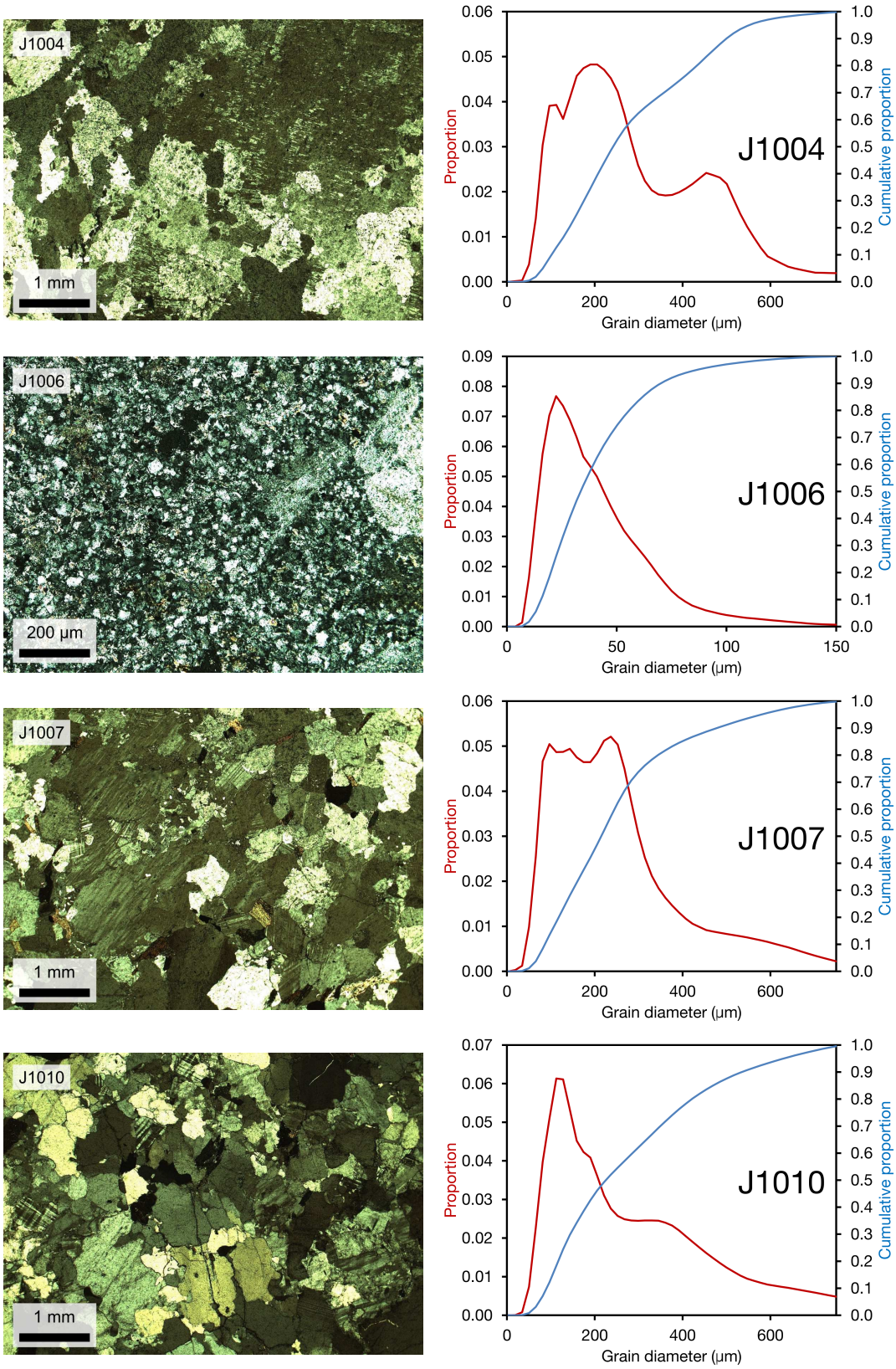

Figure S4: Petrographic thin sections and grain size analysis using DGS (Buscombe, 2013).

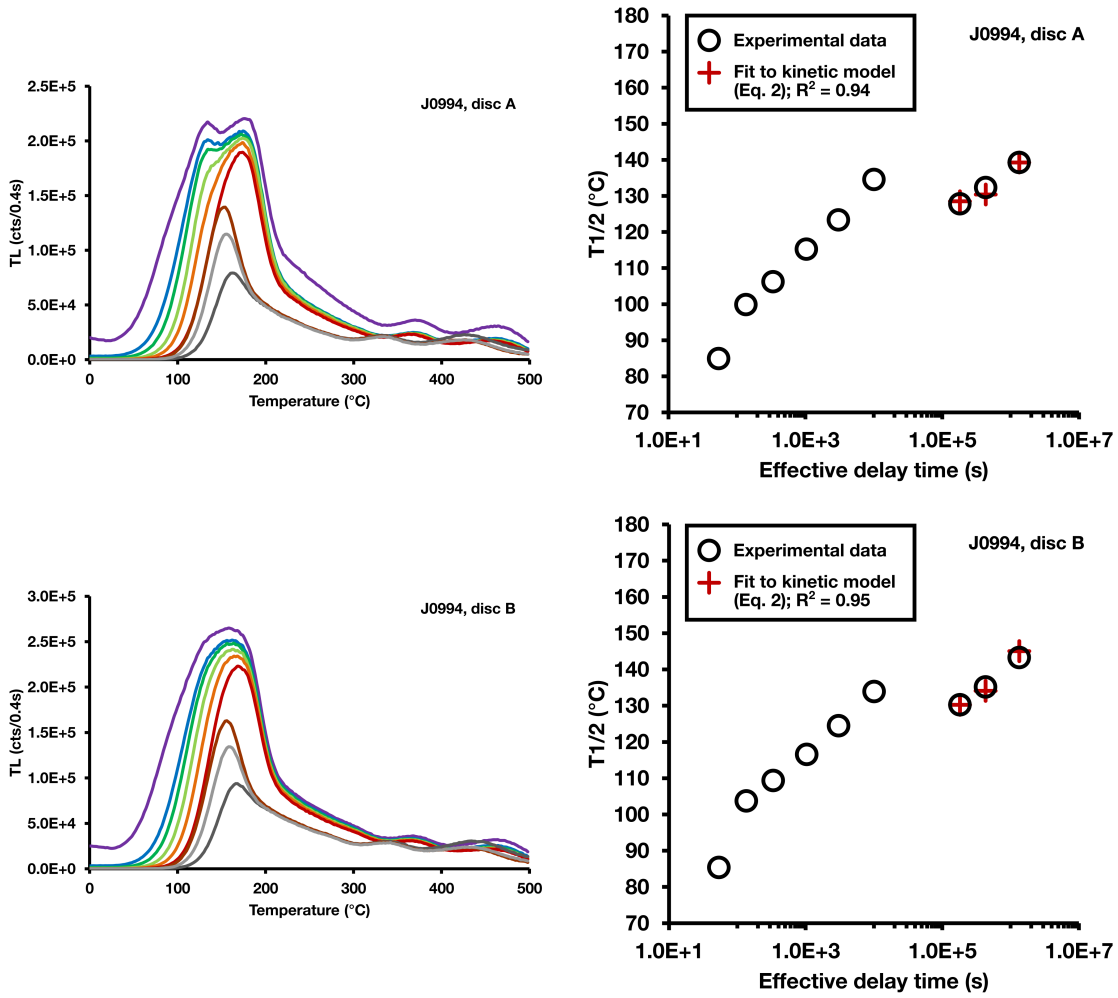

Figure S5: TL signals and $T_{1/2}$ corresponding values from sample J0994 measured after fading at room temperature for effective delay times of 54 s to 16 days.

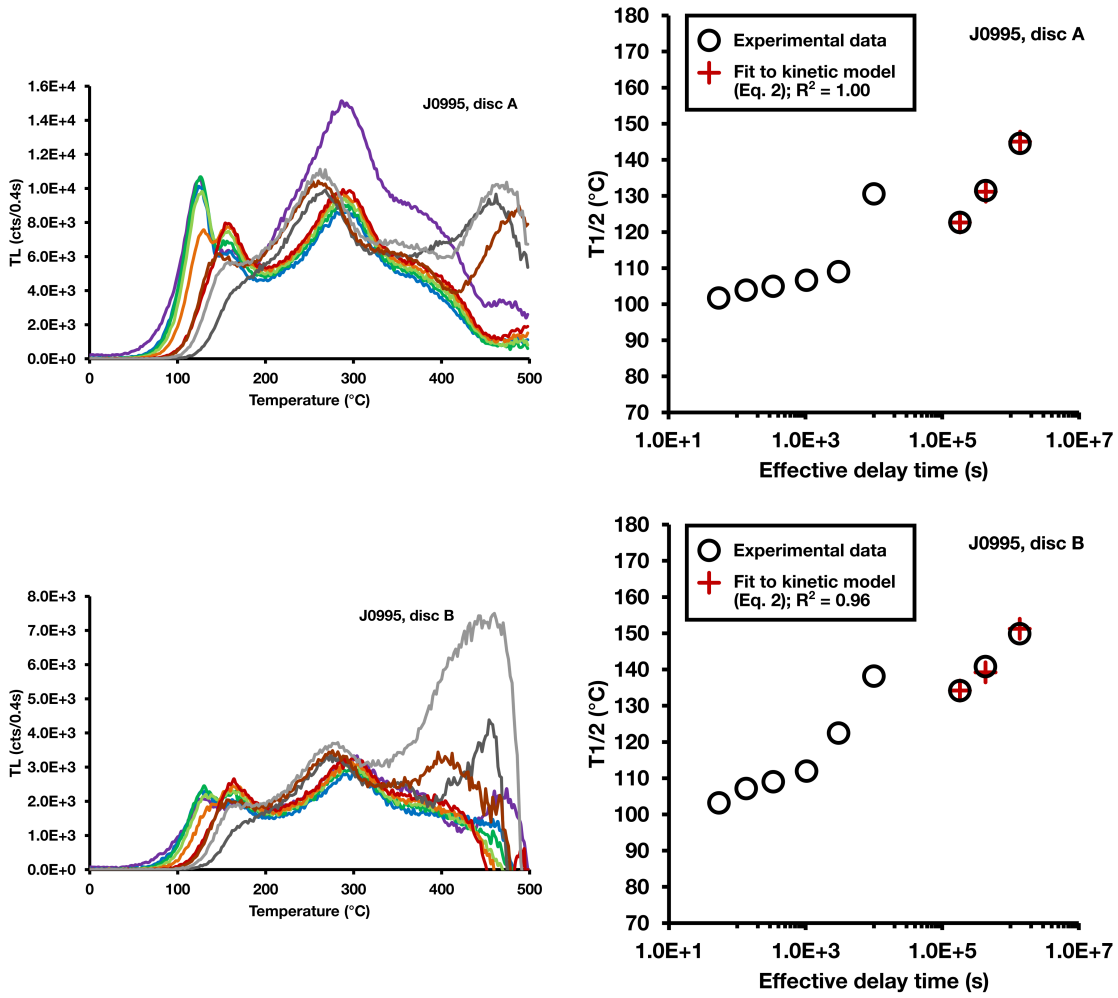

Figure S6: TL signals and $T_{1/2}$ corresponding values from sample J0995 measured after fading at room temperature for effective delay times of 54 s to 16 days.

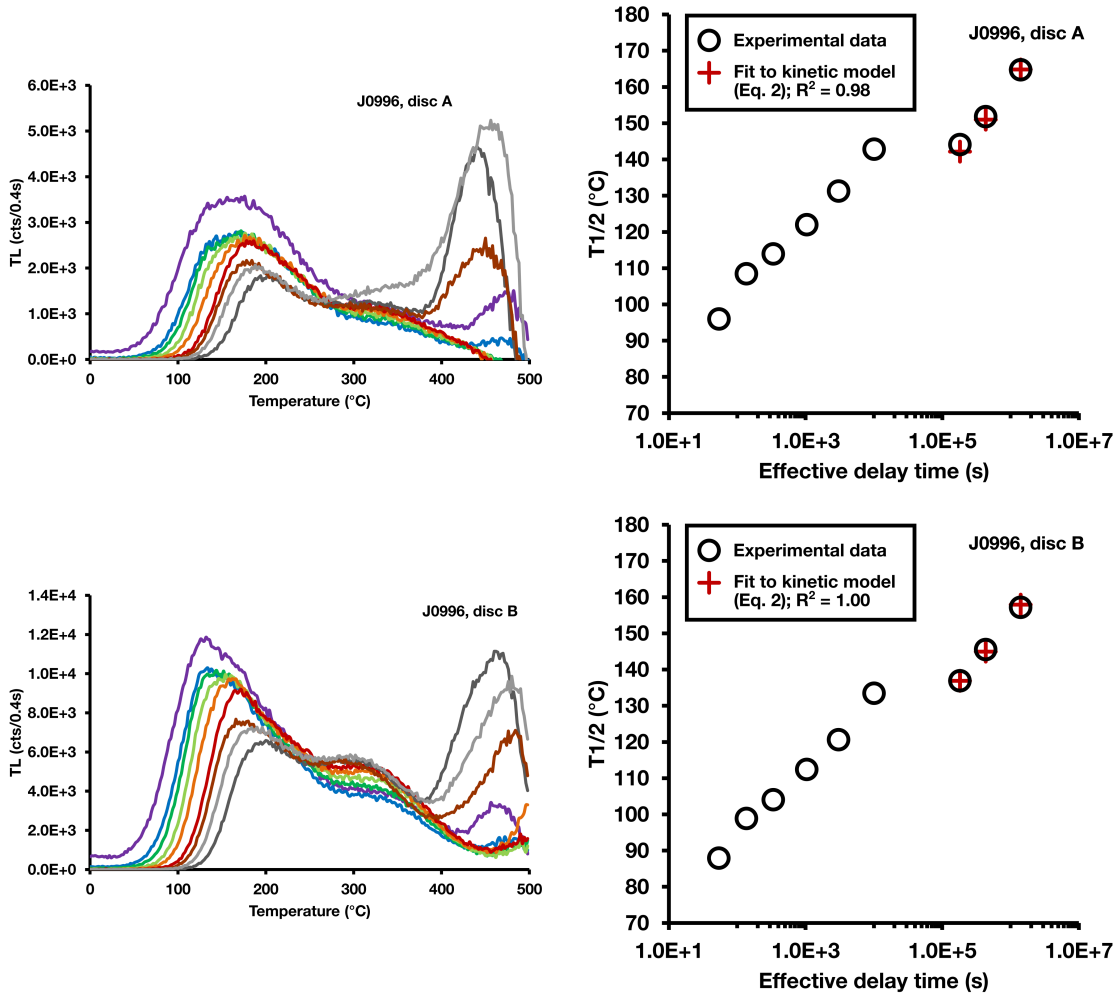

Figure S7: TL signals and $T_{1/2}$ corresponding values from sample J0996 measured after fading at room temperature for effective delay times of 54 s to 16 days.

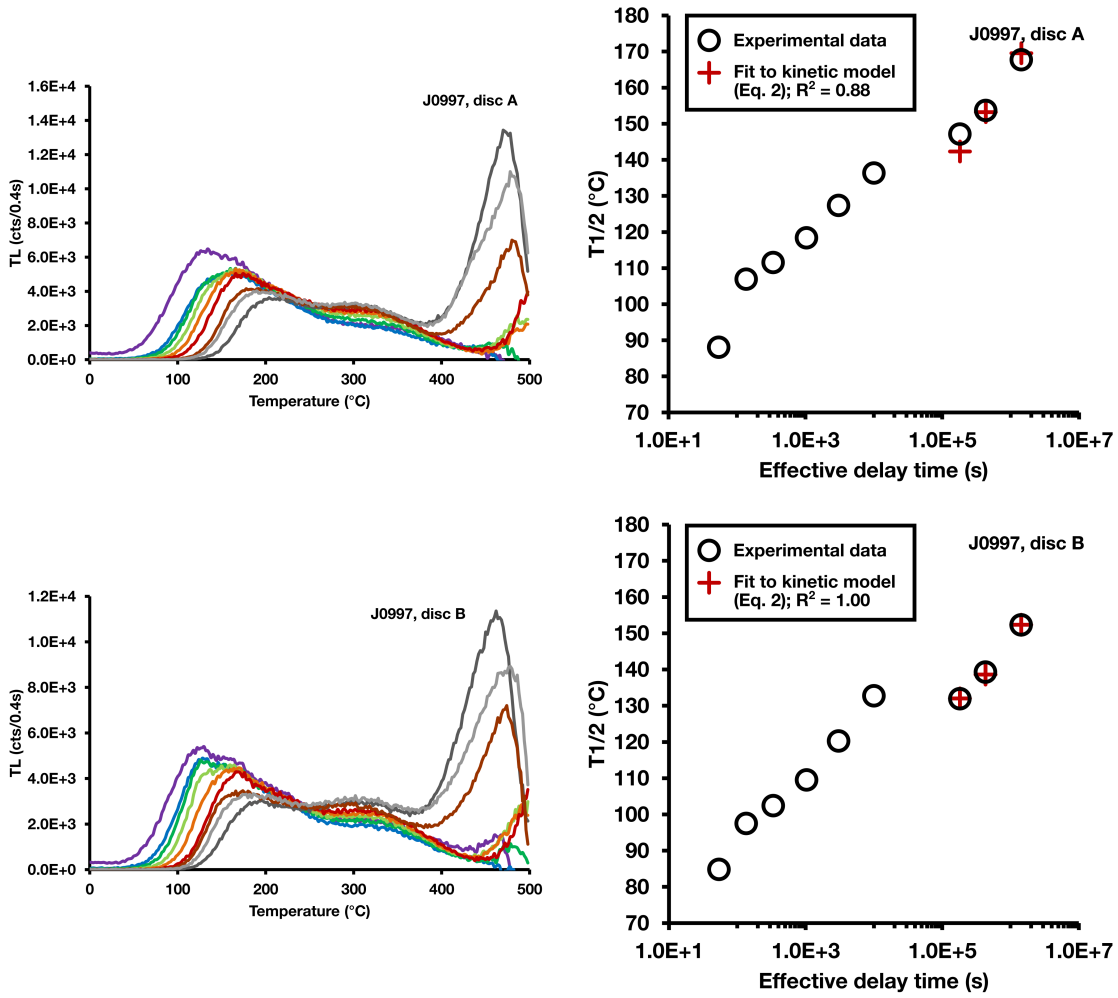

Figure S8: TL signals and $T_{1/2}$ corresponding values from sample J0997 measured after fading at room temperature for effective delay times of 54 s to 17 days.

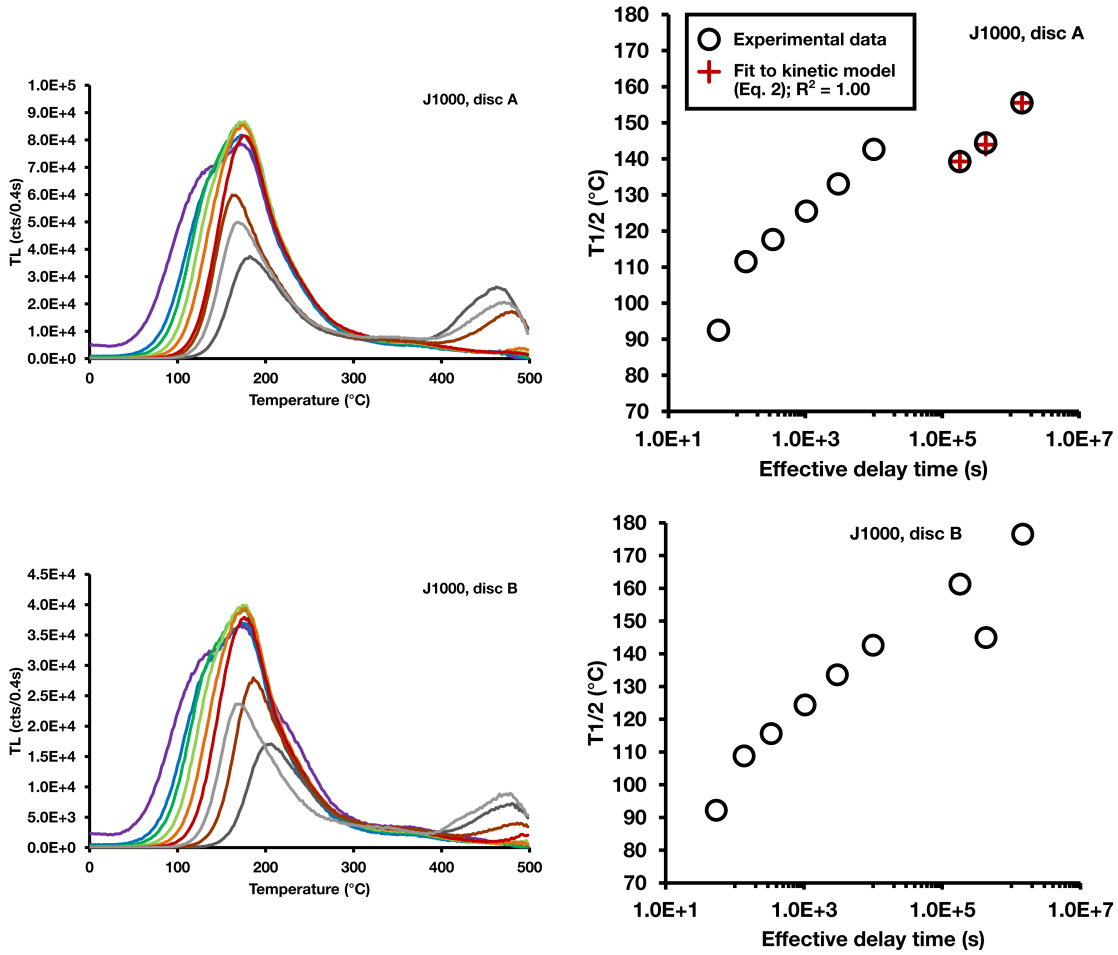

Figure S9: TL signals and $T_{1/2}$ corresponding values from sample J1000 measured after fading at room temperature for effective delay times of 54 s to 17 days.

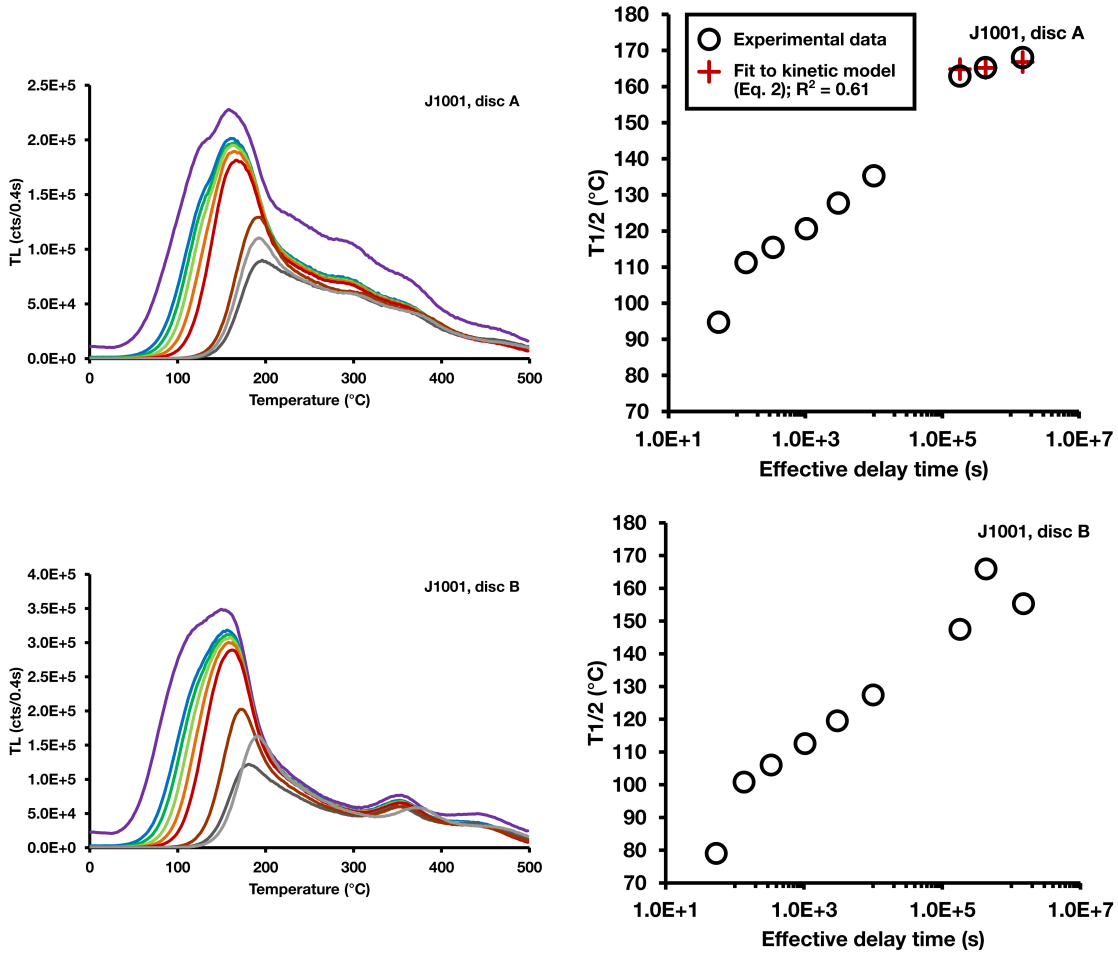

Figure S10: TL signals and $T_{1/2}$ corresponding values from sample J1001 measured after fading at room temperature for effective delay times of 54 s to 17 days.

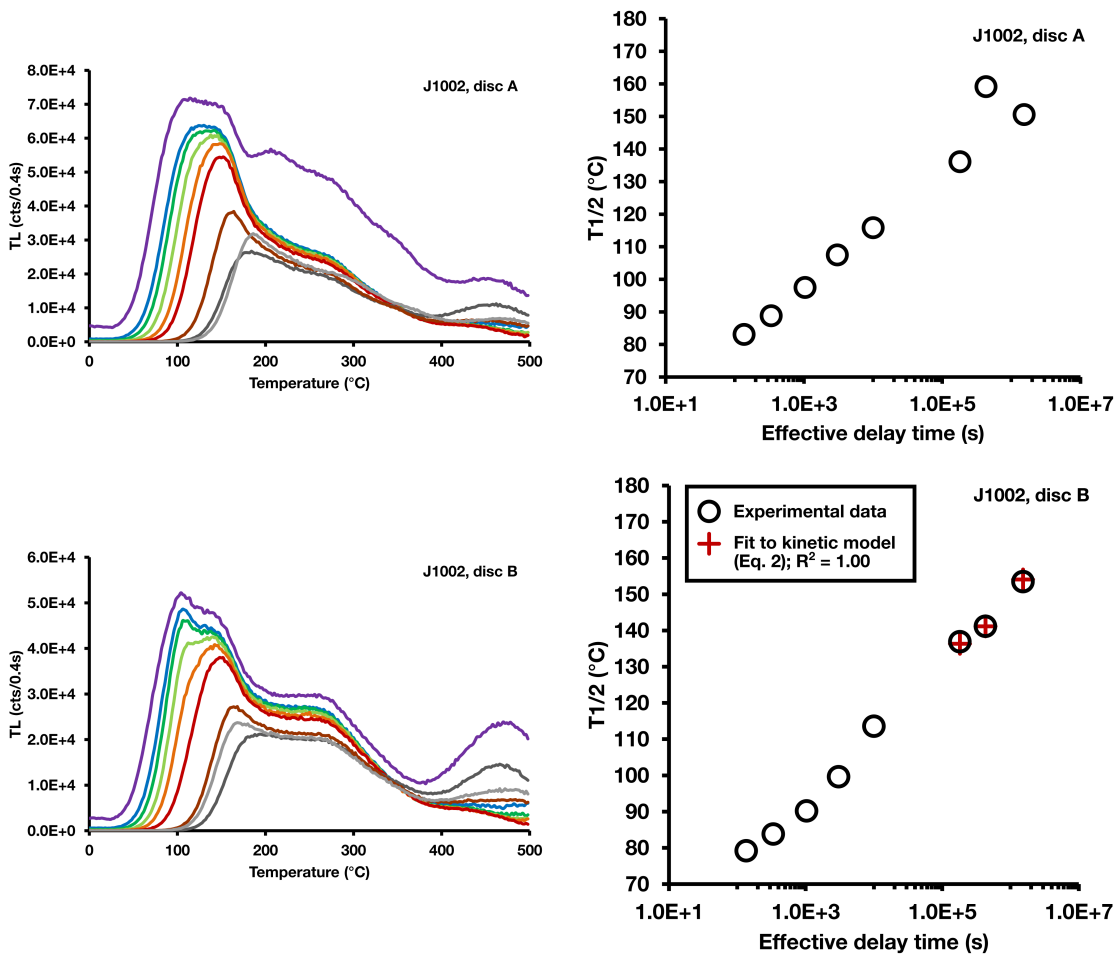

Figure S11: TL signals and $T_{1/2}$ corresponding values from sample J1002 measured after fading at room temperature for effective delay times of 54 s to 18 days.

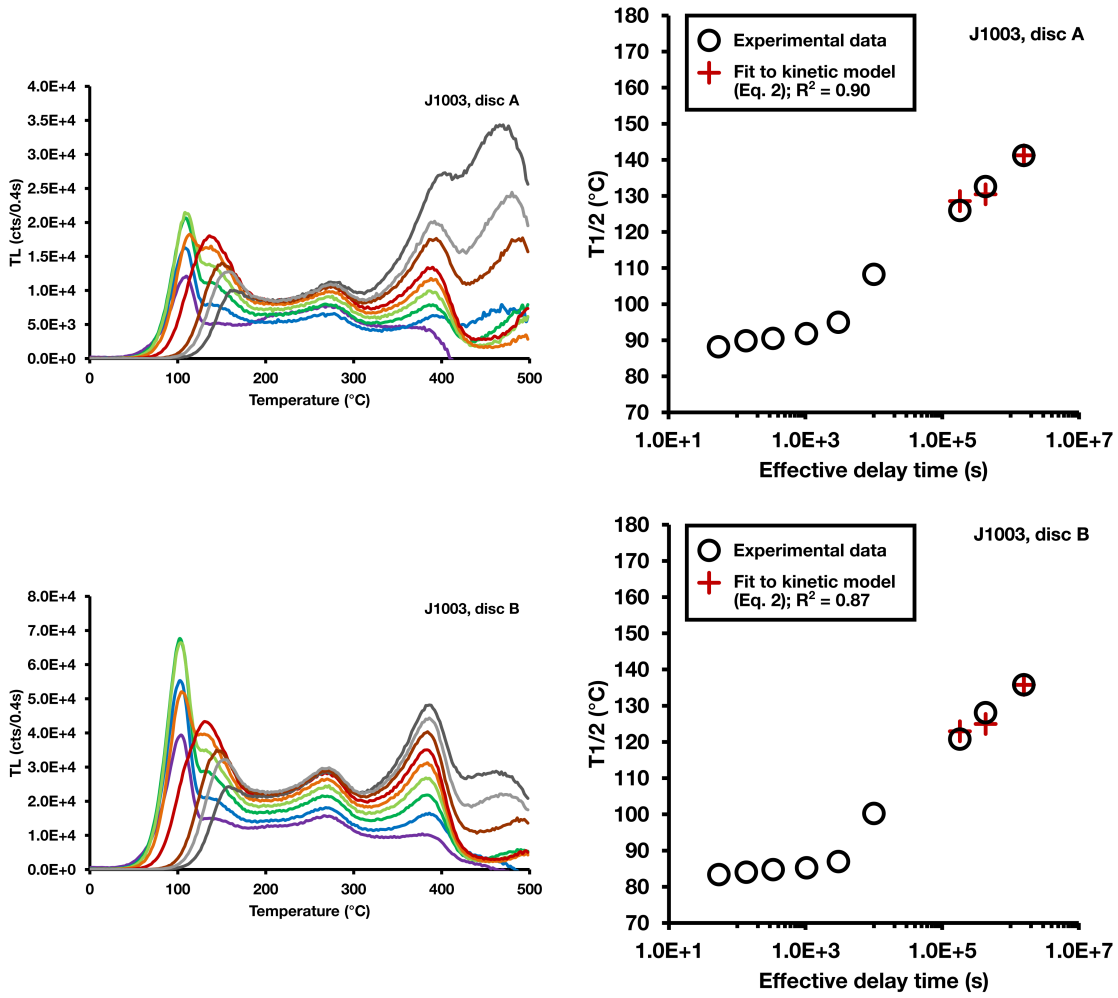

Figure S12: TL signals and $T_{1/2}$ corresponding values from sample J1003 measured after fading at room temperature for effective delay times of 54 s to 18 days.

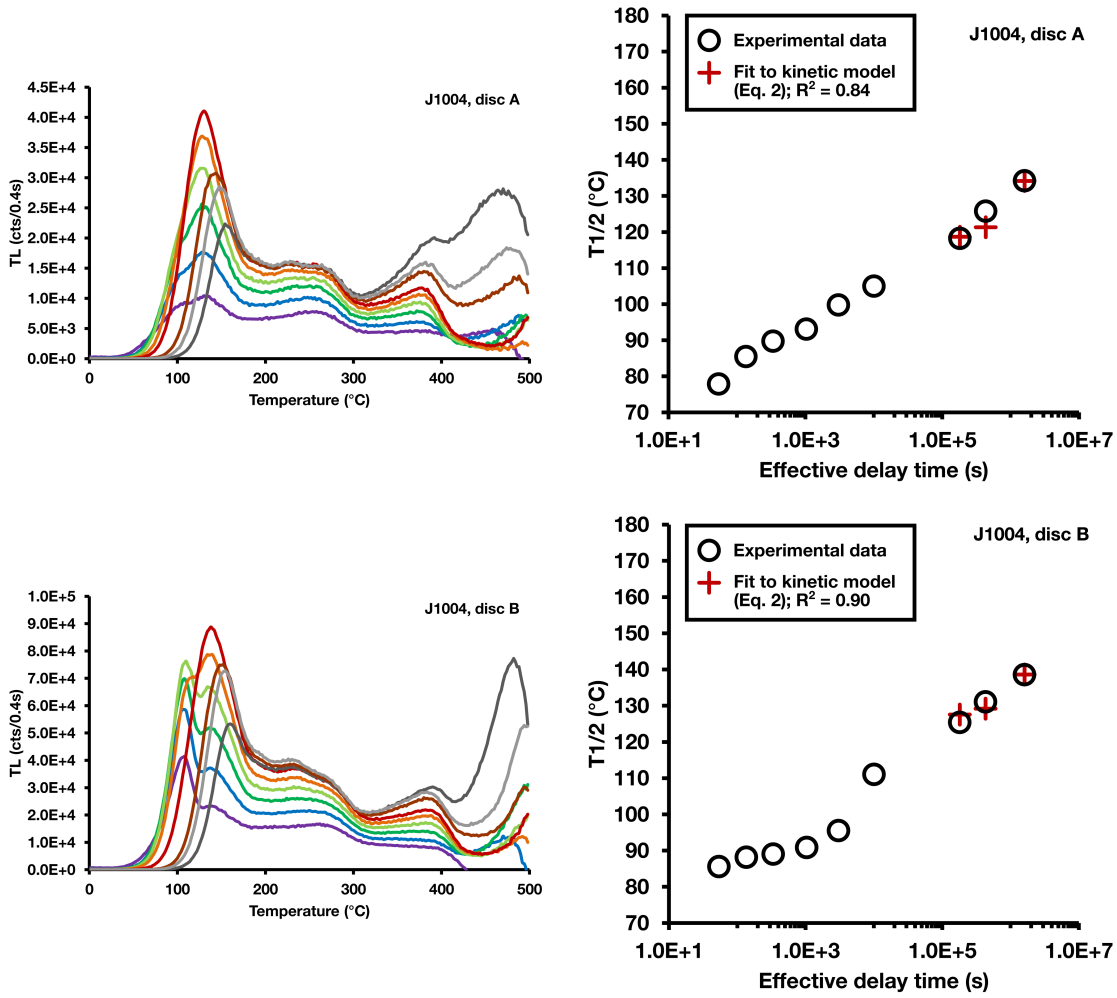

Figure S13: TL signals and $T_{1/2}$ corresponding values from sample J1004 measured after fading at room temperature for effective delay times of 54 s to 19 days.

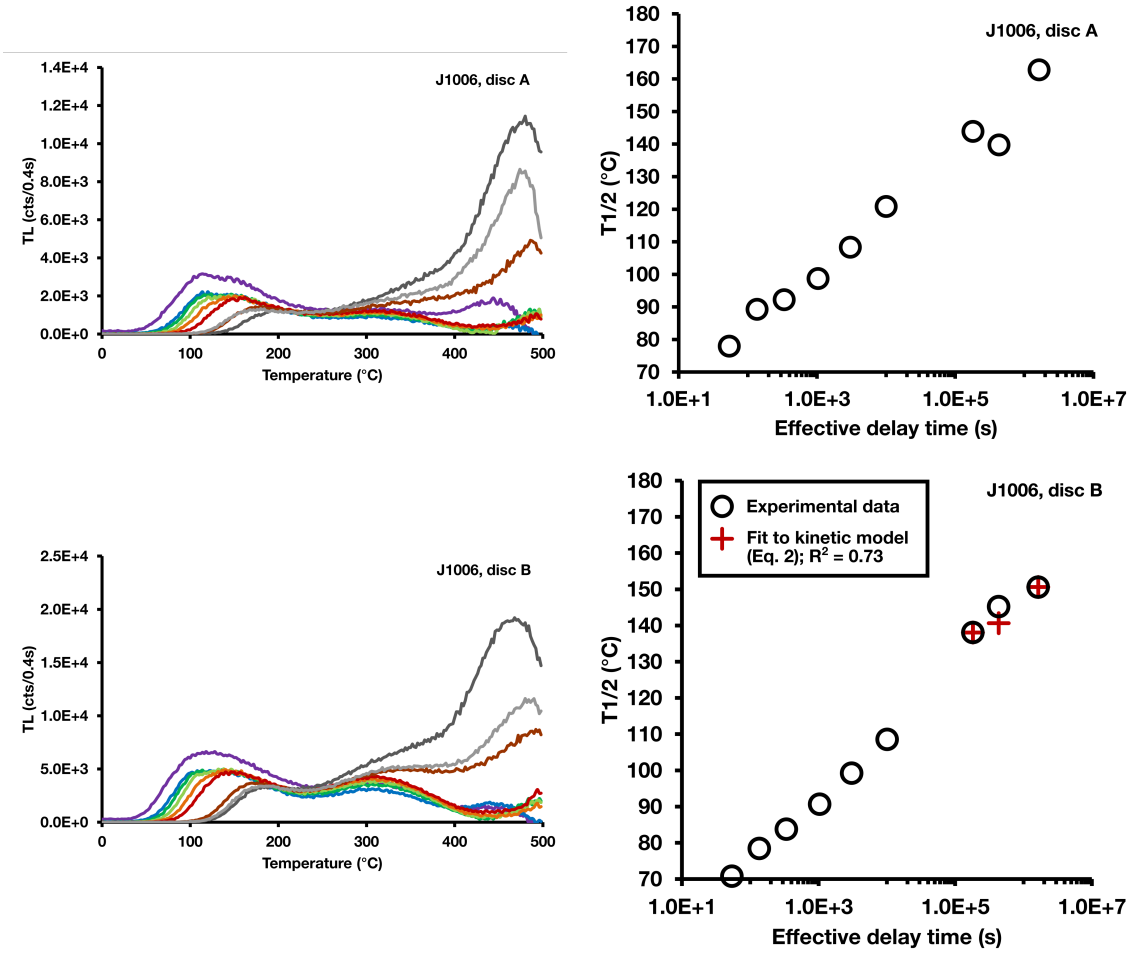

Figure S14: TL signals and $T_{1/2}$ corresponding values from sample J1006 measured after fading at room temperature for effective delay times of 54 s to 19 days.

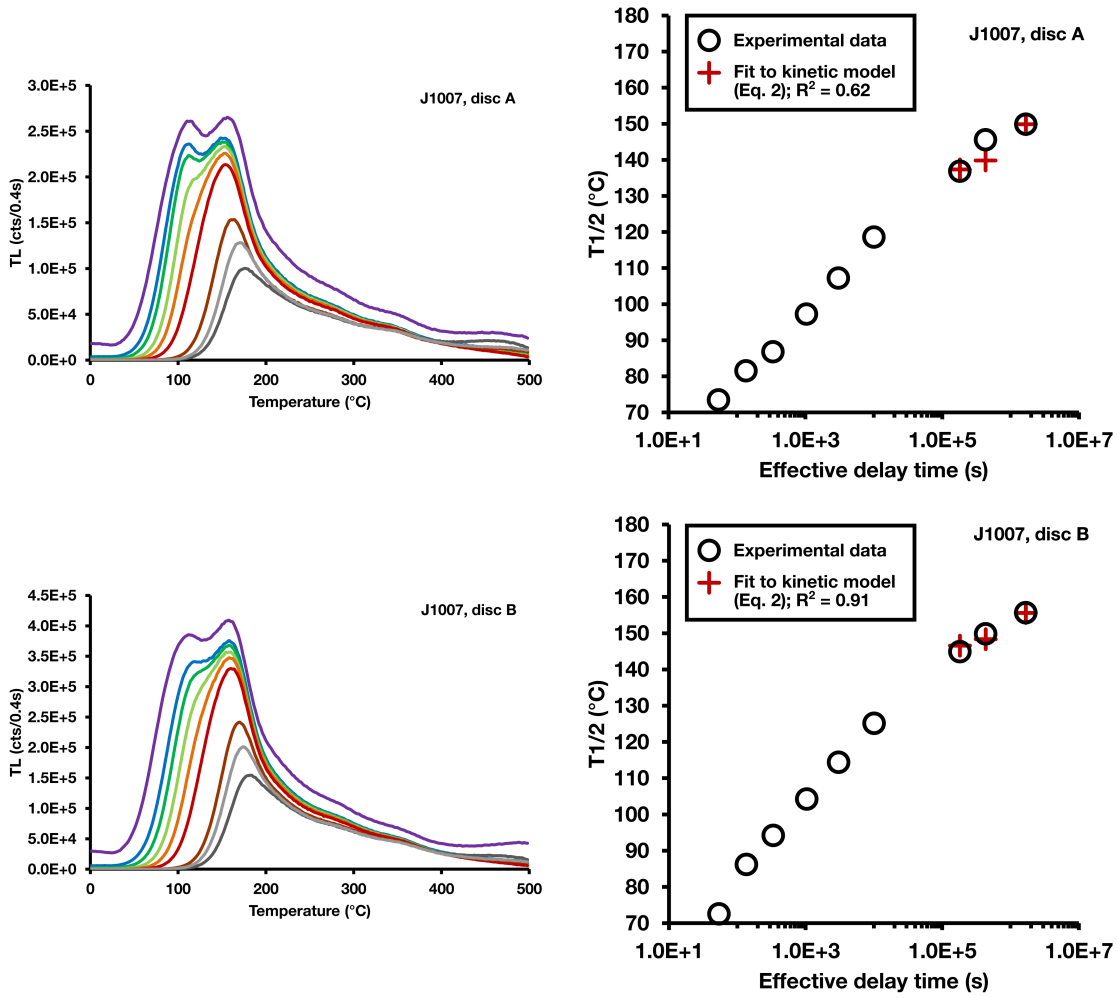

Figure S15: TL signals and $T_{1/2}$ corresponding values from sample J1007 measured after fading at room temperature for effective delay times of 54 s to 19 days.

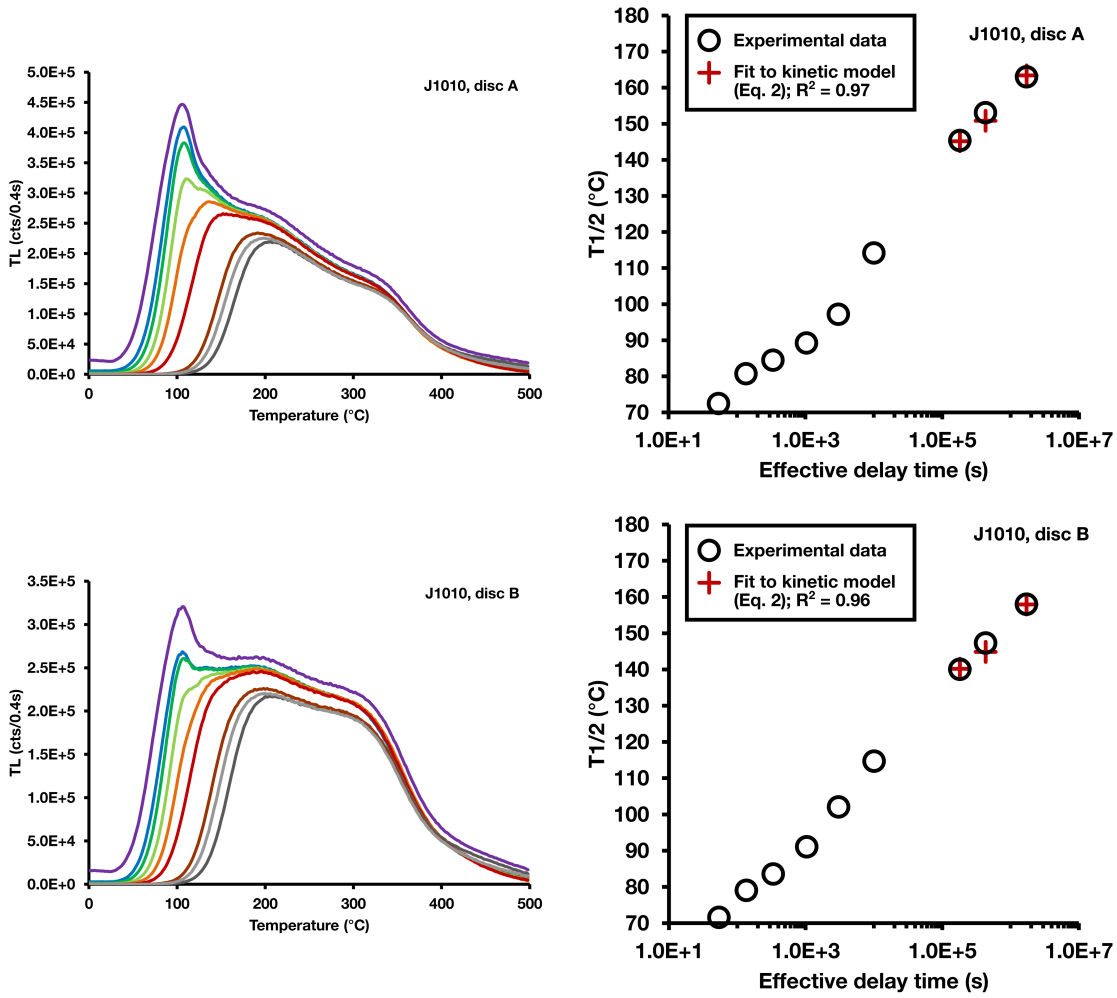

Figure S16: TL signals and $T_{1/2}$ corresponding values from sample J1010 measured after fading at room temperature for effective delay times of 54 s to 20 days.